Equation of state of a granular gas homogeneously driven by particle rotations

Eric Falcon, Jean-Claude Bacri, Claude Laroche

Equation of state of a granular gas homogeneously driven by particle rotations

E. Falcon[(a)], J.-C. Bacri and C. Laroche

Univ Paris Diderot, Sorbonne Paris Cité, MSC, UMR 7057 CNRS, F-75 013 Paris, France, EU

PACS 45.70.-n – Granular system
PACS 05.20.Dd – Kinetic theory
PACS 75.50.-y – Studies of specific magnetic materials

Abstract. - We report an experimental study of a dilute "gas" of magnetic particles subjected to a vertical alternating magnetic field in a 3D container. Due to the torque exerted by the field on the magnetic moment of each particle, a spatially homogeneous and random forcing is reached where only rotational motions are driven. This forcing differs significantly from boundary-driven systems used in most previous experimental studies on non equilibrium dissipative granular gases. Here, no cluster formation occurs, and the equation of state displays strong analogy with the usual gas one apart from a geometric factor. Collision statistics is also measured, and shows an exponential tail for the particle velocity distribution. Most of these observations are well explained by a simple model, and enable to better understand out-of-equilibrium systems uniformly "heated".

Introduction. – Granular gases display striking properties compare to molecular gases: cluster formation at high enough density [1–3], anomalous scaling of the pressure [2, 3] and of the collision frequency [4], non-Gaussian distribution of particle velocity [5]. These differences are mainly ascribed to dissipation occurring during inelastic collisions between particles. A continuous input of energy is thus required to reach a non equilibrium steady state for a granular gas. This is usually performed experimentally by vibrating a container wall or the whole container. For such vibration-fluidized systems, the role of the boundary condition affects the shape of the particle velocity distribution [5], as well as the extent of energy nonequipartition [6]. A spatially homogeneous forcing, driving each particles randomly, is thus needed to probe the validity domain of granular gas theories, but is hardly reachable experimentally [7]. Here, we experimentally report the equation of state and the collision statistics of a spatially homogeneous driven granular gas in a 3D container. Magnetic particles subjected to a magnetic field oscillating in time are used to homogeneously and randomly drive the system by injecting rotational energy in each particle. Rotational motions are transferred in translational ones by the collisions with the boundaries or particles. To our knowledge, this type of forcing has been only used to investigate the pattern formation of magnetic particles either in a 2D cell or suspended on a liquid surface [8], as well as the velocity distribution of magnetic particles in a 2D cell [9]. Beyond direct interest in out-of-equilibrium statistical physics, granular medium physics, and geophysics (such as dust clouds or planetary rings [10]), our study provide insight into applied problems such as magnetic hyperthermia for medical therapy [11] or electromagnetic grinders in steel mills [12], both being based on control of magnetic particle dynamics by alternating magnetic field.

Experimental setup. – The experimental setup is shown in Fig. 1. A cylindrical glass container, 10 cm in diameter and 14 cm in height, is filled with N magnetic particles, with $2 \leq N \leq 60$ corresponding to less than 1 layer of particles at rest. Magnetic particles are made of a disc permanent magnet (0.5 cm in diameter and $e = 0.2$ cm in thickness) encased in a plexiglass cylinder (d=1 cm in outer diameter, 0.25 cm in thickness, and $L = 1$ cm long), both axes being collinear (see pictures in Fig. 1). This configuration enables a reduction of a factor 38 of the dipole-dipole interaction between two particles. The magnetic induction of this dipolar particle, $\mu_0\mathcal{M} = 250$ G is measured by a Hall probe at the top of the cylinder, $\mathcal{M}$ being the magnetization of the particle, and $\mu_0 = 4\pi 10^{-7}$ H/m. Its magnetic moment is

[(a)] Corresponding author: eric.falcon@univ-paris-diderot.fr

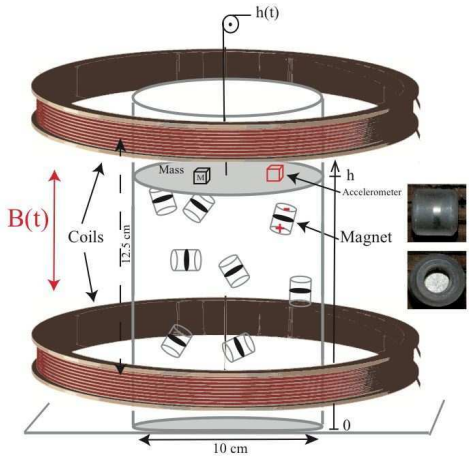

Fig. 1: (Color online) Experimental set up. Right insets shows pictures of a magnetic particle (1 cm scale).

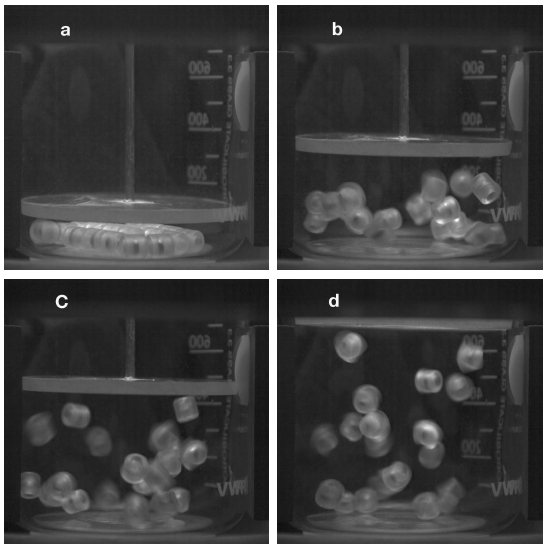

Fig. 2: (Color online) Snapshots of magnetic granular gas. $N = 20$. (a) Initial conditions: $B = 0$, a plexiglass lid is laying on the particles. When B is increased from (b) to (d), a gas-like regime develops and the lid rises up due to the collision of magnetic particles on it. For full evolution, see movie N20onset.m4v

$\mathsf{m} \equiv \mathcal{M}V_p$ with $V_p = \pi d^2 L/4 = 0.78$ cm^3 the volume of a particle. The container is placed between two coaxial coils, 18 cm (40 cm) in inner (outer) diameter, 12.5 cm apart, the container and the coil axes being collinears as in Fig. 1. A 50 Hz ac current is supplied to the coils in series by a variable autotransformer (Variac 260V/20 A). An ac vertical magnetic induction B is thus generated in the range $0 \leq B \leq 225$ G with a frequency $f = 50$ Hz. Due to the Helmholtz configuration of the coils, B is spatially homogeneous within the container volume with a 3% accuracy. Motions of particles are visualized with a fast camera (Photron Fastcam SA1.1) with a 250 fps or a 500 fps. An accelerometer stuck on the lid records the collision frequency and the impact amplitude on the lid during 500 s, the sampling frequency being 100 kHz to resolve collisions (~ 60 μs). We focus here on the dilute regime with volume fractions of $0.2\% \leq NV_p/V \leq 8\%$, with V the volume of the container. The particle mean free path is $l \equiv d/(NV_p/V) \gtrsim 0.1$ m, and the Knudsen number $Kn \equiv l/h \gtrsim 1$.

Forcing mechanism. – Assume θ the angle between the vertical field $B(t) = B \sin \omega t$ and a magnetic moment of a particle m. A torque $\mathsf{m} \times B$ is thus exerted by the field on the magnetic moment of each particle. The angular momentum theorem writes $Id^2\theta(t)/dt^2 = \mathsf{m}B \sin \omega t \sin \theta$, with $I = m(3d^2/4 + L^2)/12 = 0.14$ g cm^2 the moment of inertia of the particle, and $m = 1$ g the particle mass. This equation is known to display periodic motions, period doubling, and chaotic motions [13]. The ratio between the magnetic dipolar energy, $E_d = \mathsf{m}B$, and the rotation energy at the field frequency, $E_{rot} = I\omega^2/2$ controls the stochasticity degree. The synchronization between the angular frequency of the particles and the magnetic field one, ω, is predicted to occur when $E_d \ll E_{rot}$, that is $B \ll I\omega^2/(2\mathsf{m}) = 493$ G. When this condition is violated, as it is the case for our range of B, chaotic rotational motions occur [13] as it is shown for a single particle in the movie N1.m4v. The external magnetic field thus generates an erratic rotational driving of each particle. A spatially homogeneous forcing is thus obtained where only the rotational degrees of freedom of each particle are erratically driven.

Gas-like regime. – N particles are placed at the bottom of the container, their axes being in the horizontal plane, normal to B (see Fig. 2a). A plexiglass lid lays on the particles, its mass being balanced by a counterweight. When B is increased, a transition occurs at a critical B_c where particles begin to jump and lift up the lid. We found that $B_c = 75 \pm 5$ G whatever N. When B is further increased a stationary gas-like regime is observed with particles rotating and translating erratically - see Fig. 2b-d and movie N20onset.m4v. We observe that the axis of rotation of most particles is normal to the particle axis in order to align the direction of its magnetic moment with the vertical oscillating magnetic field. The frequency and direction of the particle rotation are erratic, showing unpredictably reversing. Their angular frequencies are thus not synchronized with the forcing frequency, $\omega = 2\pi f$. The stationary gas-like regime at fixed B is illustrated for $N = 10$ and $N = 20$ in the movies N10.m4v and N20.m4v slowed down 100 times and 12.5 times, respectively.

Method. – Measurements are performed as follows. A mass M is added on the lid ($0.82 \leq M \leq 10$ g with a 0.82 step) and the lid is stabilized due to the collision of particles at a height that depends on B (constant-pressure experiment). The height $h(t)$ reached by the lid exhibits fluctuations in time around a mean height $\langle h \rangle$ as shown in the inset of Fig. 3. $h(t)$ is measured by an angular

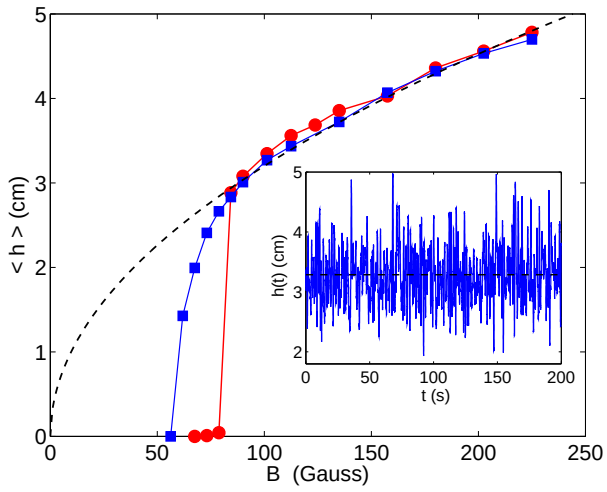

Fig. 3: (Color online) Hysteretic evolution of $\langle h \rangle$ for an increasing (•) and decreasing (■) magnetic field B. $N = 10$, $M = 4.7$ g. Dashed line is $\langle h \rangle \sim B^{1/2}$. Inset: Typical temporal evolution of $h(t)$ for $B = 101$ G, $N = 10$ and $M = 4.7$ g. Dashed line is $\langle h \rangle$=3.3 cm.

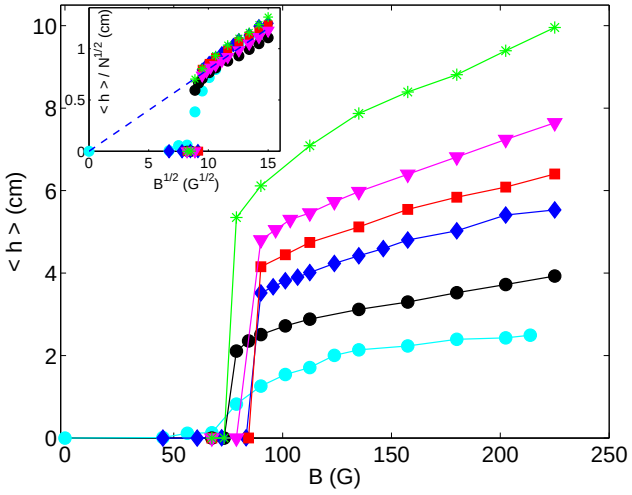

Fig. 4: (Color online) $\langle h \rangle$ vs. increasing B for different particle numbers $N = 4, 10, 15, 20, 30$ and 40 (from bottom to top). $M = 6.9$ g. Inset: best rescaling $\langle h \rangle / N^{1/2}$ vs. $B^{1/2}$. Dashed line has a slope 0.08 cm/G$^{1/2}$.

position transducer (12.3 mm/V sensitivity) at a 200 Hz sampling frequency during 200 s, the sensor output voltage being linear with the angle, and h. Note that the results reported here are unaffected when performing constant-volume experiments (the lid height is kept constant by adding a mass on the lid that depends on B).

Fluidization onset. – The mean height $\langle h \rangle$ reached by the lid is shown in Fig. 3 as a function of B for fixed N and M. The onset of the particle fluidization is hysteretic, occurring at B_c^i for increasing B, and at $B_c^d < B_c^i$ for decreasing B. One finds $B_c^d = 56 \pm 1$ G and $B_c^i = 75 \pm 5$ G whatever N. The thresholds come from the balance between magnetic energy, E_m, of a particle and the gravity energy, $E_g = mgd$, needed to vertically move it over its diameter, d, where g is the acceleration of gravity. When B is decreased, E_m corresponds to the particle dipolar energy, $E_d = \mathsf{m}B$, and one finds $B_c^d = mgd/\mathsf{m} \simeq 63$ G. When B is increased, particles are initially in contact, and E_m is the sum of the dipole-dipole interaction energy of two particles in contact, $E_{dd} = \mu_0 \mathsf{m}^2/(12V_p)$ [14], and the dipolar energy of a single particle E_d. By balancing $E_{dd} - E_d$ with E_g, one has $B_c^i - B_c^d = \mu_0 \mathcal{M}/12 \simeq 21$ G as found experimentally. The hysteresis is thus due to the additional field needed to separate two particles initially in contact. One has also $E_d/E_{dd} = 12B/(\mu_0 \mathcal{M}) \gg 1$ for $B \gg B_c$.

State equation. – Far from the onset, Fig. 3 shows that $\langle h \rangle$ scales as $B^{1/2}$ meaning that the gaseous regime expands more and more when B increases. For fixed M, $\langle h \rangle$ is shown in Fig. 4 as a function of B for different particle numbers N. The larger N is, the higher is the height reached by the lid for a fixed B. The best rescaling is displayed in the inset of Fig. 4, and shows that $\langle h \rangle / N^{1/2} \sim B^{1/2}$. For fixed N, $\langle h \rangle$ is shown in Fig. 5 as a function of B for different added mass M on the lid. The larger M is, the smaller is the height reached by the lid for a fixed B. The best rescaling is displayed in the inset of Fig. 5, and shows that $\langle h \rangle M^{1/2} \sim B^{1/2}$. To sum up, one finds an experimental state equation for the magnetic granular gas

$$M \langle h \rangle^2 = kNB \ , \qquad (1)$$

where $k = 0.05$ g cm^2/G is a constant.

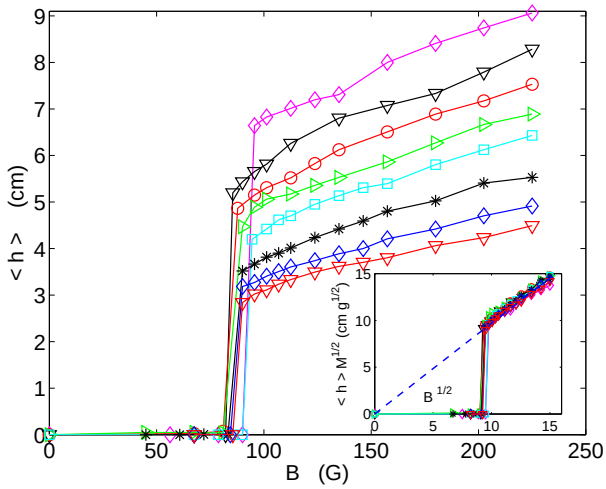

Fig. 5: (Color online) $\langle h \rangle$ vs. increasing B for different masses added $M = 2.3$, 3.1, 3.9, 4.7, 5.3, 6.9, 8.6 and 10 g (from top to bottom). $N = 15$. Inset: best rescaling $\langle h \rangle / M^{1/2}$ vs. $B^{1/2}$. Dashed line has a slope 0.97 cm g$^{1/2}$/G$^{1/2}$.

Model. – Due to the stochastic forcing, a fraction of the magnetic energy is continuously injected in each particle. Since an out-of-equilibrium stationary state is reached, the injected energy is dissipated in average dur-

ing collisions. Although the dissipated energy involved rotational and translational parts, both can be assumed to be proportional [16]. Thus, the balance between magnetic energy and translational kinetic energy dissipated during collisions leads to $v^2 \sim \mathsf{m}B$. Thus, the typical particle velocity, scales as

$$v(B) \sim \sqrt{B} \ . \tag{2}$$

More precisely, assuming simple collision rules (i.e. with no rotation) for the sake of simplicity, the energy loss by a particle of mass m during a collision with the lid of mass M is $\frac{mv^2}{2}(1-\epsilon^2)\frac{M}{m+M}$, ϵ being the particle-boundary restitution coefficient. The energy balance finally leads to $v \sim \sqrt{\mathsf{m}B\frac{m+M}{mM(1-\epsilon^2)}}$.

Let us now model the fact that the lid motion under gravity is stabilized at an altitude h due to the particle collisions. One thus balances τ_l, the time of flight under gravity of the lid subjected to particle collisions, and τ, the time of flight of particles between 2 collisions *with the lid* at the altitude h. One has $\tau_l = v_l/g$ with v_l the lid velocity, and $\tau = 2h/v$ for $N = 1$. For N particles, the collision frequency, $1/\tau$, has to enhance by a large particle density, and a large scattering cross section ($\sim V_p$). It thus makes sense to divide τ by the volume fraction NV_p/V, with $V = Sh$, S being the container area. Then, one has

$$\tau = \frac{2h^2 S}{Nv(B)V_p} \ . \tag{3}$$

Balancing τ_l with τ then leads to $h^2 = Nvv_lV_p/(2gS)$. The lid velocity is $v_l = v(1+\epsilon)\frac{m}{m+M}$ from simple inelastic collision rules. Thus, using the expressions for h^2, v_l and v, the theoretical state equation reads $Mgh^2 \sim NB(\frac{V_p}{S})$ in good agreement with the experimental one of Eq. (1). For a more accurate description, complex inelastic collision rules should be included [15, 16] since linear and angular particle velocities are coupled.

Collision statistics. – Additional experiments have been performed with the lid fixed to an altitude h. A typical temporal recording of the accelerometer is shown in the bottom inset of Fig. 6. Each peak corresponds to the acceleration undergoes by a particle during its collision on the lid. The acceleration peak amplitude, A, and the time lag, τ, between two successive collisions on the lid are randomly distributed. A thresholding technique is applied to the signal to detect the collisions [4]. Figure 6 shows that the mean time lag scales as $\overline{\tau} = \kappa h^2/\left(NB^{1/2}\right)$ with $\kappa = 0.18$ s G$^{1/2}$/cm^2 over 2 decades when varying one single parameter h, B or N while keeping the other two fixed. This result is in good agreement with the model of Eqs. (2) and (3). Another experimental verification of Eq. (2) is as follows. The mean amplitude of acceleration peaks is experimentally found to scale as $\overline{A} \sim h^0 N^0 B^{1/2}$ as shown in Fig. 7. For an impulse response of the accelerometer to a single collision, the product of the acceleration peak amplitude, A, times the duration of the collision, δt,

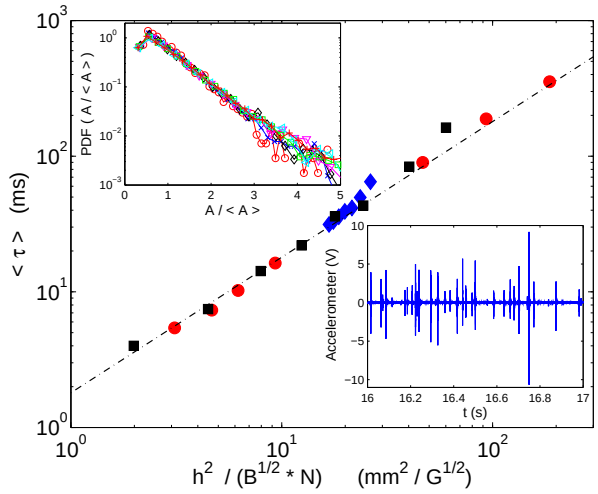

Fig. 6: (Color online) Bottom inset: Temporal signal of the accelerometer showing 35 collisions in 1 s ($N = 10$, $h = 5$ cm, $B = 157$ G). Main: $\overline{\tau}$ vs. $h^2/(N\sqrt{B})$ for: (•) $1 \le N \le 60$ ($B = 180$ G, $h = 5$ cm), (♦) $90 \le B \le 222$ G ($N = 10$, $h = 5$ cm), and (■) $2 \le h \le 11$ cm ($N = 15$, $B = 180$ G). Dot-dashed line has a unit slope. Top inset: PDF($A/\overline{A}$) for $90 \le B \le 222$ G ($N = 15$, $h = 5$ cm).

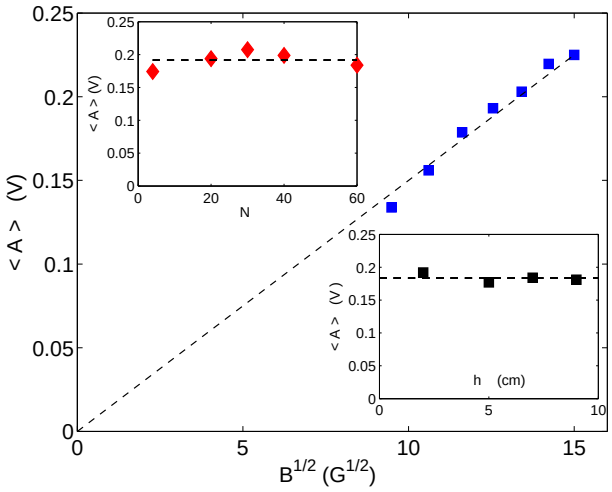

Fig. 7: (Color online) Experimental scaling of the mean particle velocity near the wall obtained from the accelerometer measurements. Main: $\overline{A}$ vs. $\sqrt{B}$ for $N = 15$, and $h = 6$ cm. Top inset: $\overline{A}$ vs. N for $B = 180$ G, and $h = 6$ cm. Bottom inset: $\overline{A}$ vs. h for $B = 180$ G, and $N = 15$.

is equal to the magnitude of the particle velocity v, and thus $v = A\delta t$ ($\delta t \simeq 60\mu s$ is roughly constant). One has thus $\overline{v} \sim B^{1/2}$ in agreement with Eq. (2). The translational granular temperature near the wall thus scales as $T_w \sim h^0 N^0 B^1$.

For various B at fixed N, the probability density functions (PDF) of A show exponential tails that collapse on a single curve when rescaled by $\overline{A}$ (see top inset of Fig. 6). Similar results are found at fixed B whatever N. Moreover, since $A \sim v$, the tail of the velocity's PDF is thus

found to scale as $\exp(-c\ v/\overline{v})$ independently of the volume fraction since $\overline{v} \sim h^0 N^0 B^{1/2}$. Consistently, the time lag distribution is found to scales as $\exp(-c'\tau/\overline{\tau})$, c and c' being dimensionless constants.

Discussion. – We have obtained the equation of state of a dissipative granular gas driven homogeneously by the rotations. With usual notations (the pressure P on the lid $\sim Mg/S$, and the container volume $V = Sh$), the equation of state thus reads $PV \sim NE_c\frac{V_p}{V}$, with $E_c \sim \langle v^2\rangle \sim B$ the mean translational kinetic energy per particle of velocity v. Surprisingly, this equation is close of the equation of state of a perfect gas ($PV = NE_c$) with a geometric correction: the particle-container volume ratio. This can be partially ascribed to particle-wall interactions since the Knudsen number $Kn \gtrsim 1$. Moreover, it differs from the equation of state of a dissipative granular gas driven by a vibrating wall $PV \sim E_c$ with $E_c \sim \mathcal{V}^{\theta(N)}$ with $\mathcal{V}$ the forcing velocity of the wall, and $\theta(N)$ a decreasing function from $\theta = 2$ at low N to $\theta \simeq 0$ at large N when the clustering phenomenon occurs [3]. Here, no clustering is observed even when the volume fraction is increased up to 40%. We also show that the magnetic field B in our experiment is the analogous of the thermodynamic temperature for molecular gases, or the analogous of the granular temperature for dissipative granular gases since one has $\langle v^2\rangle \sim B$. The distribution of particle velocity near the top wall displays an exponential tail and is independent of the particle density. It is thus not Gaussian as for an ideal gas, or stretched exponential and density dependent as for a boundary-forced granular gas [5]. Finally, the collision frequency $\sim 1/\langle\tau\rangle$ is found to scale as $N\sqrt{B}$. This result is consistent with the collision frequency of an ideal gas $\sim N\sqrt{\langle v^2\rangle}$, but not with the one of a vibro-fluidized dissipative granular gas in a dilute regime $\sim N^{1/2}\mathcal{V}$ [4]. This difference is related to the spatially homogeneous forcing.

Conclusion. – We have experimentally studied, for the first time, a 3D granular gas driven homogeneously in volume by particle rotations. This differs from previous experimental studies of granular gas where the energy was injected by vibration at a boundary. The equation of state is experimentally identified and the collision statistics measured (scaling of the particle rms velocity and the mean collision frequency with the forcing). Several differences are reported with respect to thermodynamiclike gas and/or non equilibrium vibro-fluidized dissipative granular gas: (i) the gas-like state equation has a geometric correction (container-particle aspect ratio), (ii) no cluster formation occurs at high density, and (iii) the particle velocity distribution displays an exponential tail. The use of this new type of forcing will be of primary interest to experimentally test the possible equipartition of rotational and translational energy, a feature not guaranteed for out-of-equilibrium systems [17].

* * *

We thank C. Wilhelm and F. Gazeau for fruitful discussions. This work has been supported by ESA Topical Team on granular materials N°4000103461.

REFERENCES

[1] Kudrolli A., Wolpert M. and Gollub, J. P., *Phys. Rev. Lett.*, **78** (1997) 1383
[2] Falcon E. *et al.*, *Phys. Rev. Lett.*, **83** (1999) 440
[3] Falcon E., Fauve S., and Laroche C., *Eur. Phys. J. B*, **9** (1999) 183; McNamara S. and Falcon E., *Phys. Rev. E*, **71** (2005) 031302.
[4] Falcon E. *et al.*, *EPL*, **74** (2006) 830
[5] Rouyer F. and Menon N., *Phys. Rev. Lett.*, **85** (2000) 3676; Losert W. *et al.*, *Chaos*, **9** (1999) 682; Olafsen J. S. and Urbach J. S., *Phys. Rev. E*, **60** (1999) R2468; Kudrolli A. and Henry J., *Phys. Rev. E*, **62** (2000) R1489; vanZon J. S. *et al.*, *Phys. Rev. E*, **70** (2004) 040301(R); Wang H.-Q., Feitosa K. and Menon N., *Phys. Rev. E*, **80** (2009) 060304(R)
[6] Wang H.-Q. and Menon N., *Phys. Rev. Lett.*, **100** (2008) 158001
[7] Cafiero R., Luding S. and Hermann H. J., *EPL*, **60** (2002) 854
[8] Snezhko A., Aranson I. S. and Kwok W.-K., *Phys. Rev. Lett.*, **94** (2005) 108002; *Phys. Rev. E*, **73** (2006) 041306
[9] Schmick M. and Markus M., *Phys. Rev. E*, **78** (2008) 010302(R); Bologa K. K., Syutkin S. V. and Serditov V. N., *Magnetohydrodynamics*, **18** (1982) 24
[10] Goldreich P. and Tremaine S., *Icarus*, **34** (1978) 227; Bridges F. G., Hatzes A. and Lin D. N. C., *Nature*, **309** (1984) 333
[11] Fortin J.-P. *et al.*, *J. Am. Chem. Soc.*, **129** (2007) 2628; Gazeau F., Lévy M., and Wilhelm C., *Nanomedecine (Lond.)*, **3** (2008) 831
[12] Lupanov A. P. *et al.*, *Technical Physics*, **52** (2007) 954
[13] Croquette V. and Poitou C., *J. Phys. Lett.*, **42** (1981) 537; Meissner H. and Schmidt G., *Am. J. Phys.*, **5** (1985) 800.
[14] Rosensweig R. E., *Ferrohydrodynamics* (Dover, New York) 1997
[15] Huthmann M. and Zippelius A., *Phys. Rev. E*, **56** (1997) R6275
[16] Brilliantov N. V., Pöschel T., Kranz W. T. and Zippelius A., *Phys. Rev. Lett.*, **98** (2007) 128001
[17] Nichol K. and Daniels K. E., *Phys. Rev. Lett.*, **108** (2012) 018001